

## Towards quantum well hot hole lasers

P. Kinsler\* and W. Th. Wenckebach

*Department of Applied Physics,  
Faculty of Applied Sciences, T.U. Delft,  
Lorentzweg 1, 2628 CJ Delft, The Netherlands.*

It should be possible to improve hot-hole laser performance by moving from bulk materials to a quantum well structure. The extra design parameters enable us to alter the band structure by changing the crystal orientation of the growth direction; to use the well width to shift the subband offsets, enabling the effect of the LO phonon scattering cut-off to be controlled; and to use modulation doping to ensure a high hole concentration to increase the gain without the dopants being present in the gain region. We present the first simulations of THz quantum well hot-hole lasers that can produce inversion and optical gain.

## I. INTRODUCTION

Hot hole lasers [1, 2] emit in the THz (far-infrared) with an unusually broad gain spectrum, allowing amplification and generation of laser pulses on a picosecond time scale. The THz band has important potential applications in (e.g.) medical imaging and office communications. Bulk hot-hole lasers have been realised in p-Ge, producing gains of  $\sim 0.25\text{cm}^{-1}$  around 4THz. Of the III-V materials, both GaAs and InSb are suitable for hot hole lasers; although their performance is not as good as in Ge [3]. Investigation of these is the most useful for industrial applications because of the existing ability to grow high quality III-V structures.

We present a discussion of likely modes of operation of quantum well hot-hole lasers in GaAs, together with predictions from Monte Carlo simulations for one design. The simulations use an infinite-well  $k.p$  bandstructure, and include optical phonons, acoustic phonons, and piezoelectric phonons [4–6]. As yet they do not include ionised impurity scattering, but this is a small effect and should not affect the character of the results significantly.

## II. QUANTUM WELLS

Bulk hot-hole lasers can be described using the heavy and light hole valence bands: an electric field accelerates the heavy holes in a streaming motion to high energies  $E > E_{LO}$ ; from where (ideally) they scatter into light hole cyclotron orbits formed by the magnetic field; and then emit a photon and return to low energy in the heavy hole band to repeat the cycle. In a quantum well each valence band breaks up into a set of subbands: heavy hole subbands HH1, HH2, HH3, ...; and similarly for light holes LH1, LH2, etc. The non parabolicity of the bulk bandstructure leads to a variety of possible quantum well bandstructures, depending on the orientation of the crystal axes in the well material. Figure 1 shows the lower subbands of two simple cases schematically. Note that the [101] well is not symmetric in  $x$  and  $y$ ; and that for the [001] well the HH dispersions are no longer even approximately parabolic,

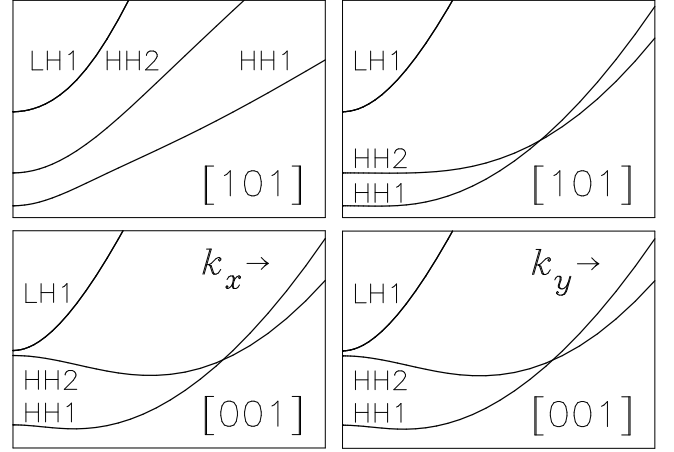


FIG. 1: Band structure of a quantum well hot-hole laser. Upper graphs: 100Å well with a [101] growth direction; lower graphs: a 100Å well with a [001] growth direction. The  $k_x$  variation is shown on the left-hand graphs, and  $k_y$  on the right. The vertical scale is 0–100meV, and the horizontal 0– $1 \times 10^9 \text{m}^{-1}$ .

with the HH2 having a noticeable local maximum at the origin.

The [101] well has two heavy-hole subbands (HH1, HH2) that need to be considered. For wells over about 50Å wide, the two lowest energy, and hence most heavily populated subbands will be HH1 and HH2. This means that in contrast to the bulk case we do not need a magnetic field to confine the light holes in cyclotron orbits. The LH1 is well above the HH2 for a 100Å well, and so has minimal effect on hot-hole laser operation. Along one direction ( $y$ ) both HH subbands are very flattened at the base, but with a LH-like curvature for larger  $k_y$ ; whereas along the other ( $x$ ) HH2 sits between HH1 and LH1. This means that the heavy-hole distributions will be roughly rectangular in outline; and an increasing electric field will shift the distributions along its direction. In the  $x$  direction the two HH subbands (nearly) cross at a point about 15meV above the bottom of HH1, allowing for fast inter-subband scattering. Holes that get further up HH1 to an energy equal to  $E_{LO}$  above the bottom of HH2 will quickly emit an LO phonon and return to populate either HH2 or HH1. Note that HH2 is flat to larger  $k_y$  values than HH1, making it relatively easy to get inversion where HH2 is flat but HH1 is not.

\*Electronic address: Dr.Paul.Kinsler@physics.org

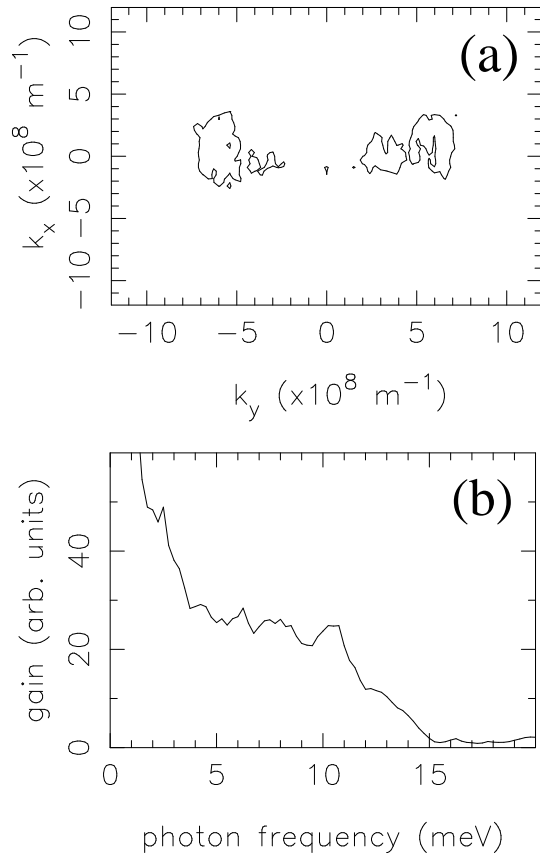


FIG. 2: [101] 100Å quantum well hot-hole laser, with electric field  $F_x = 250\text{V/cm}$  (a) Contour plot showing the region of inversion; (b) spectrum of the gain cross-section for  $y$  polarised light. Both graphs are affected by statistical noise from the simulations.

Fig. 2(a) shows the difference in the distribution functions between HH2 and HH1, for an electric field of 250V/cm along the  $x$  direction. We see regions of inversion for  $k_x \approx 0$  and  $k_y \approx 5.00 \times 10^8 \text{m}^{-1}$ . There is a small displacement in the direction of the field, and the amount of inversion decreases with increasing field strength. If the electric field is applied along the  $y$  direction, we see only one inversion peak, because the other is wiped out as the HH1 distribution is shifted underneath it; and a field applied along  $x = y$  has a similar, but not so marked, effect. Figure 2(b) shows the optical gain due to the inversion obtained and shown in (a). We see optical gain occurring over the range of energies between the small splitting at the HH1-HH2 anti-crossing ( $\approx 0\text{meV}$ ) and the separation of the subband minima ( $\approx 15\text{meV}$ ).

The [001] well HH2 subband has a distinct local maximum at  $k = 0$ ; and also LH1 is rather close to HH2, and should not be neglected. Our code does not yet allow for these more complicated dispersions, but we can see that a lasing cycle

might be as follows: A HH1 of moderate positive  $k_x$  is accelerated by an electric field  $+F_x$ , where it might scatter into HH2 near the anti-crossing. Then it will scatter back onto the inverted part of HH2, either by acoustic phonon scattering or LO phonon emission. Here it will be accelerated *backwards* past  $k = 0$  to the point of inflection ( $-k_{LHi}$ ) where the HH2 effective mass is infinite; and subsequently emit a photon and drop down to HH1, from where it will eventually scatter to moderate positive  $k_x$  and will repeat the cycle. Note that HH1 also has a local maxima, but it is smaller and has less effect; and its point of inflection where holes can collect is offset from the HH2 one, and so should not interfere with population inversion too much. In contrast to the [101] well, we expect the emission spectrum of this [001] well to be peaked and centered at  $E_{HH2}(k_{LHi}) - E_{HH1}(k_{LHi})$ , where the HH2's will accumulate.

Quantum well hot hole lasers also benefit from modulation doping. One significant source of unhelpful scattering is that due to holes scattering off either other holes or impurities. We can halve this contribution to the scattering simply by moving impurities used to add the holes to the device to outside the active region. Also, we can vary the well widths to vary the inter-subband separations to greater or less than  $E_{LO}$  to enhance or reduce optical phonon scattering as required; or even use the well's crystal orientation to adjust the densities of states (DOS) of the subbands. The [101] well has HH1, HH2 with flat  $E(k)$  in the  $k_y$  direction, leading to an enhanced density of states, hence making those regions into relatively preferred destinations for scatterings. This differs markedly from the DOS effects in bulk material [3].

### III. CONCLUSIONS

We have shown the potential for quantum well hot-hole lasers by an investigation of the possible bandstructure in combination with computer simulation. Although we have not yet explored the full parameter space of possible designs, our first attempt (the 100Å [101] quantum well) produced simulations which showed inversion over a range of electric field strengths and directions, with the optimum being for a 250V/cm field in the in-plane  $x$  direction. Further, the 100Å [001] well has a bandstructure which promises a good inversion. We aim to continue to test different designs and field combinations, including the addition of magnetic fields, in order to determine the most practical designs for experimental investigation.

**Acknowledgements:** This work is funded by the European Commission via the program for Training and Mobility of Researchers.

- [2] J. N. Hovenier, A. V. Muravjov, S. G. Pavlov, V. N. Shastin, R. C. Strijbos, and W. Th. Wenckebach, Appl. Phys. Lett. **71**, 443–445 (1997), doi:10.1063/1.119573.
- [3] P. Kinsler, W. Th. Wenckebach, J. Appl. Phys. **90**, 1692 (2001), doi:10.1063/1.1384492.
- [4] C. Moglestu, *Monte Carlo simulation of semiconductor devices*, (Chapman & Hall, London, 1993).
- [5] E.O. Kane, in *Semiconductors and Semimetals*, eds. R.K. Willardson and A.C. Beer, (Academic Press, New York, 1966), Vol. **1**, page 75.
- [6] B.K. Ridley *Quantum Processes in Semiconductors*, (Clarendon Press, Oxford, 1988).